Supporting information

to

Reduction behavior of PdO-NiO/SiO_2: how the location affects cinnamaldehyde hydrogenation

Rim C.J. van de Poll, Heiner Friedrich, Emiel J.M. Hensen

This document contains the following sections:

Extended methods S1 & S2

Figures S1 – S14

Table S1

S1 Extended XPS fitting method.

Pd 3d fitting

The PdO is fitted with two peaks separated by a set distance of 5.26 eV corresponding to the peak orbital splitting of Pd. The area ratio between the first and second peak is set to 3:2 with a peak shape of GL(30). The metallic peaks have the same peak orbital splitting and area ratio. For the metallic peak a asymmetric peak shape of type LA(1.33,2.44,69) is used. The FWHM of all 4 peaks is set to be equal.

Ni 2p fitting

The Ni 2p fit is based on two spectra. The NiO(3)-SiO_2 spectra after drying at 110 °C and after reduction at 800 °C (Figure S5). Both these spectra are fitted with the minimal number of peaks after which no discernible peaks are left in the residual error. Then the area ratio's, peak positions and FWHM ratio's are fixed for all peaks yielding a model for metallic Ni and Ni^{2+}. These two models are used to fit all spectra. Comparing the Ni spectra taken at 800 °C with a bulk reference of Ar sputtered Ni metal foil (Figure S6) and a references in the literature [1], a difference in the satellite at 858.5 eV is seen. For the reduced nanoparticles in NiO(3)-SiO_2 this satellite does not reach a maximum and the peaks are not as sharp as the references. This is most likely caused by the difference between bulk references and nanoparticles present here, changing the ratio of satellite peaks.

S2 Extended method processing of CO-IR data.

Each sample pellet is treated in the in-situ cell under the required atmosphere (art. air or 10 % H_2). Then the sample is put under vacuum and cooled down using liquid nitrogen to a temperature of -170 °C (± 4 °C). An initial measurement under vacuum is taken and then CO is dosed repeatedly using a gas loop of 25 µL and the pressure was recorded. This measurement was repeated for both an empty cell and a cell containing only silica. To process the data, the first vacuum measurement is fitted to each spectrum in the domain 2400 – 2500 cm^{-1} (a domain which is devoid of any peaks) and this is subtracted from the data. The spectra of silica and the empty cell was processed the same way. The spectra of the empty cell are first subtracted (to remove the signal of gas phase CO). This is done by subtracting for each data spectra, the corresponding empty cell spectra. A small correction is made for using the actual pressure which was recorded during the measurements. For both spectra the same amount of CO was dosed using the gas dosing loop. For the subtraction of silica, first the gas phase signal is removed from the blank silica spectra. Then analogue to the empty cell, for each data spectra the corresponding empty silica spectra is subtracted.

S1. EDX measurements

HAADF-STEM images were acquired of Pd@NiO(3)-SiO_2 and NiO(3)SiO_2 as shown in figure 2 in the main article. However, due to the very small size of the nanoparticles it could not be seen whether a Pd on NiO nanoparticle system was created. Therefore STEM-EDX measurements were attempted. The measurements were carried out on a probe corrected JEOL ARM 200F TEM operated at 200 kV equipped with a 100 mm^2 centurio SSD EDX detector. It was noticed that during EDX mapping the nanoparticles would start to move after 2-3 seconds of exposure therefore, long EDX acquisition times could not be used. Figure S1 shows a HAADF-STEM image taken before (a) and after (b) EDX acquisition and the EDX mapping itself (c-f). The before and after images show that the particles and support move due to the influence of the electron beam, therefore, the EDX mapping becomes unreliable. Additionally, the EDX mapping shows that the current mapping (10 s acquisition time, 128x128 pixels) was not enough to get sufficient Pd signal. Further dose optimization was done, however, no reliable EDX data could be obtained at the required doses for EDX analysis at high resolution.

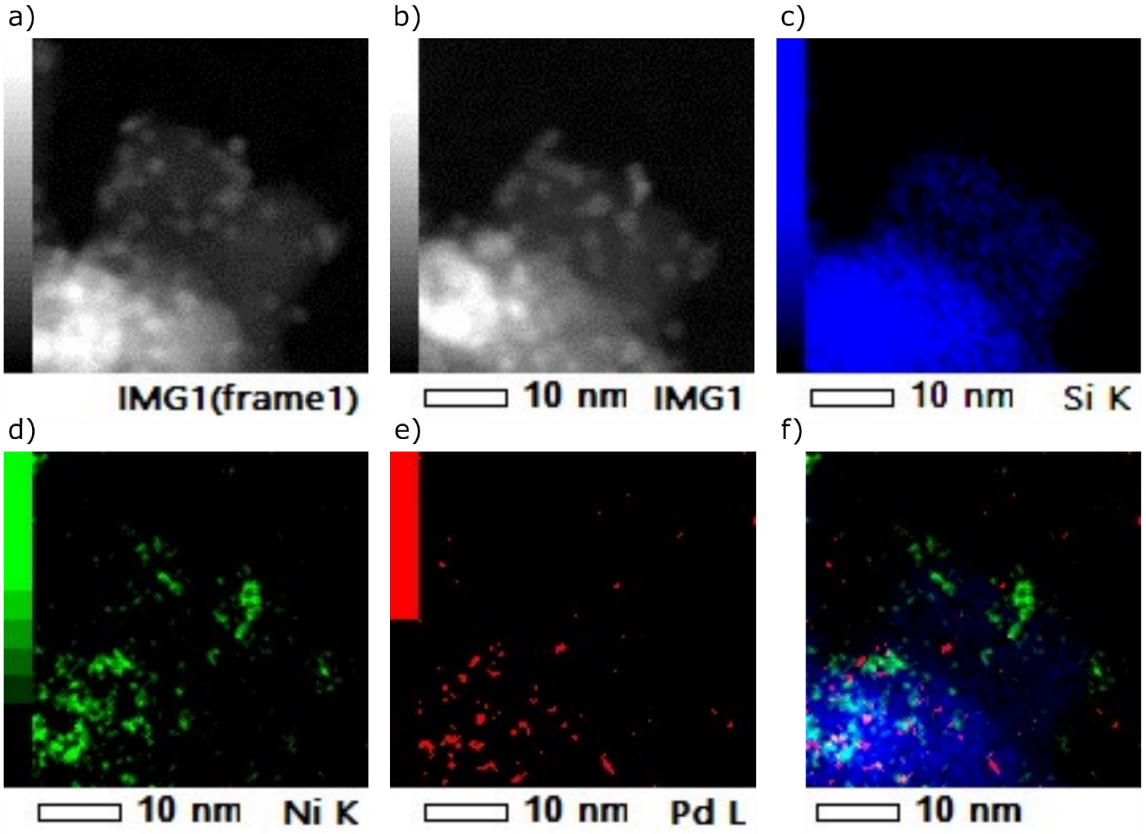

Figure S1. HAADF-STEM and EDX mapping of Pd@NiO(3)-SiO_2.

S2. Particle size distributions

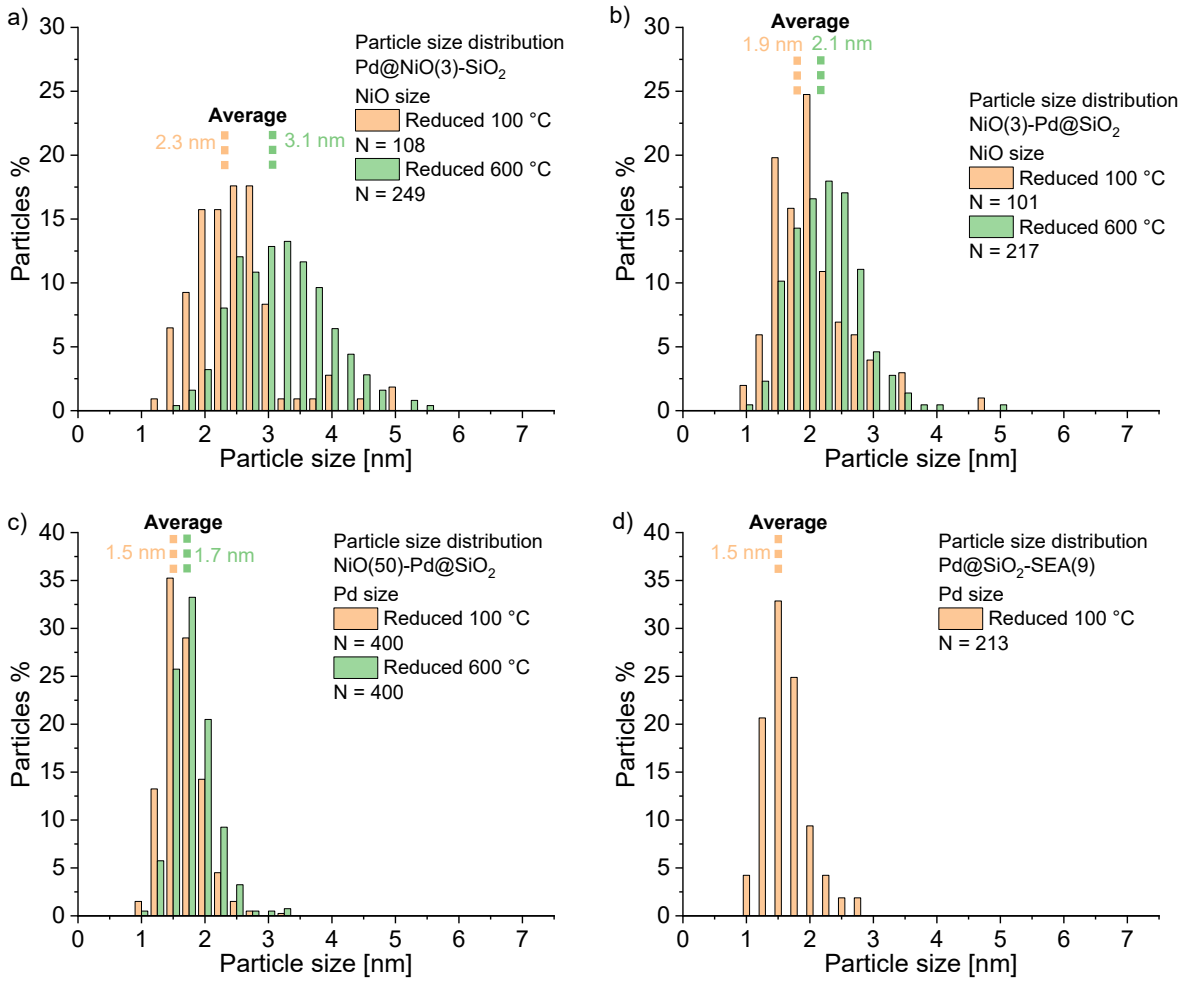

Figure S2 (a-d). Number average particle size distributions derived from HAADF-STEM images using manual annotation in ImageJ.

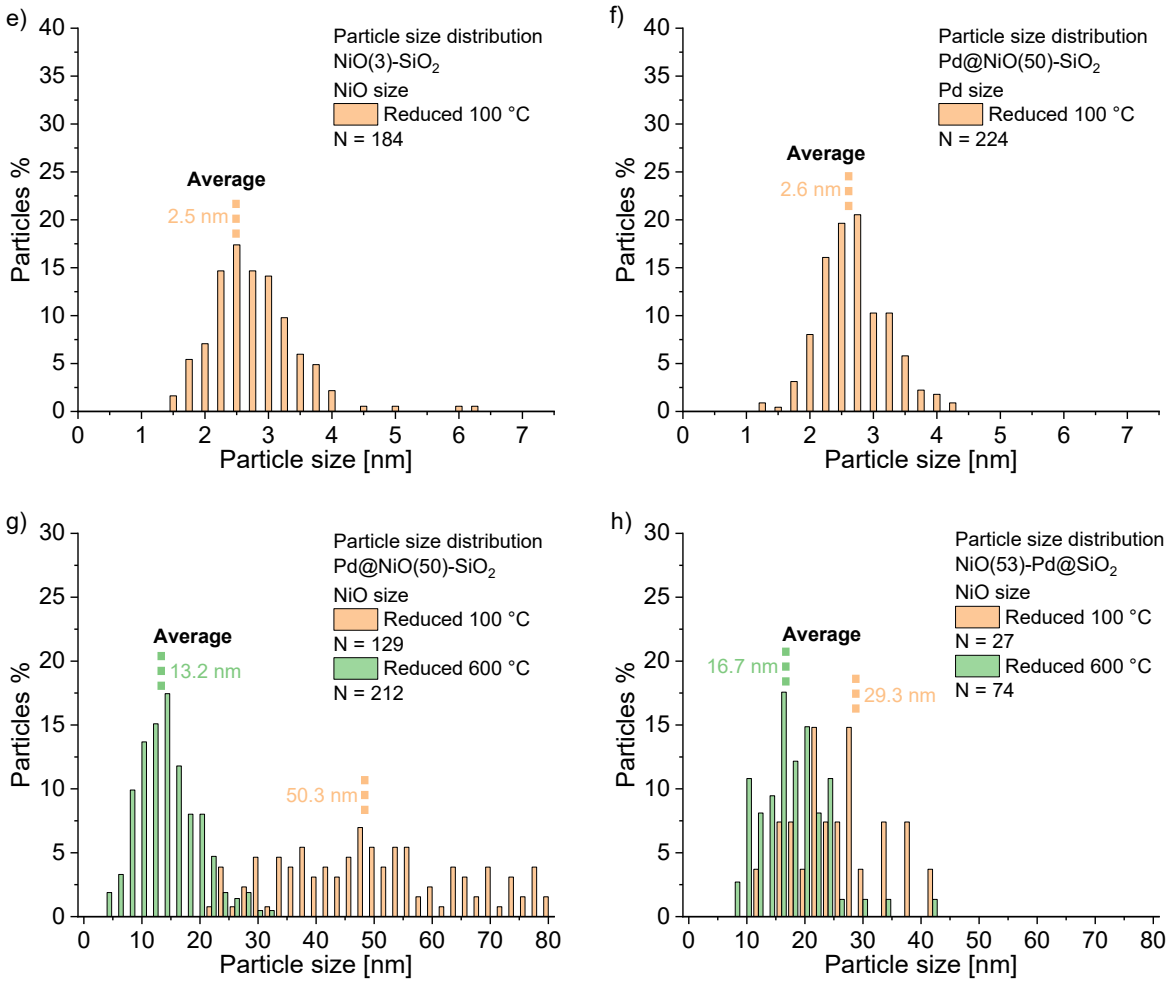

Figure S2 (e-h). Number average particle size distributions derived from HAADF-STEM images using manual annotation in ImageJ.

S3. Cinnamaldehyde hydrogenation selectivities

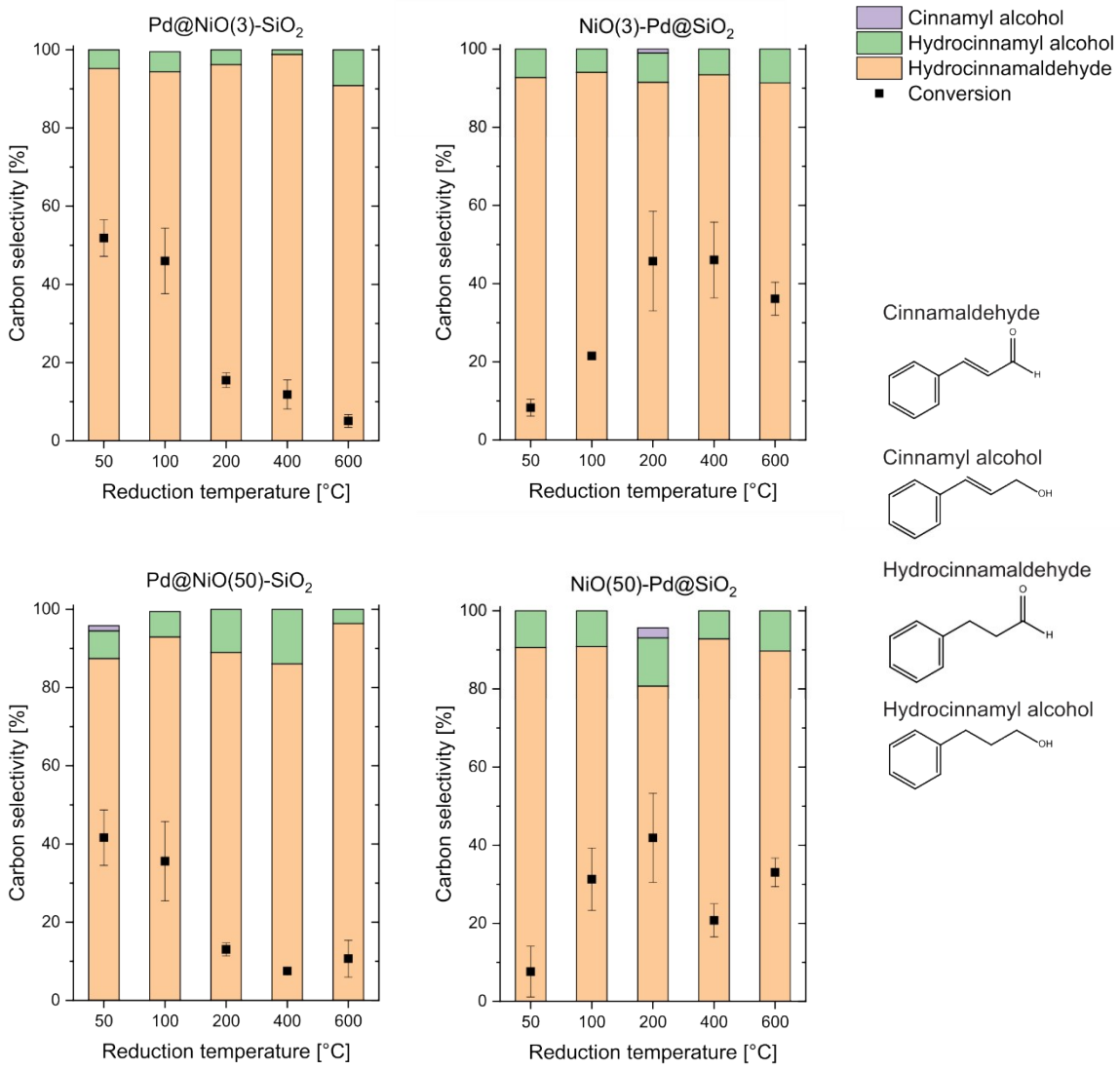

Figure S3. Cinnamaldehyde hydrogenation activity of Pd-NiO-SiO_2 catalysts (batch reactor, 50 °C, 4 mg catalyst, 2.8 ml IPA solvent, 1.2 ml cinnamaldehyde, 30 bar H_2, 10 h reaction time)

S4. Cinnamaldehyde activity of $NiO(3)\text{-}SiO_2$ and $Pd@SiO_2$ SEA 9

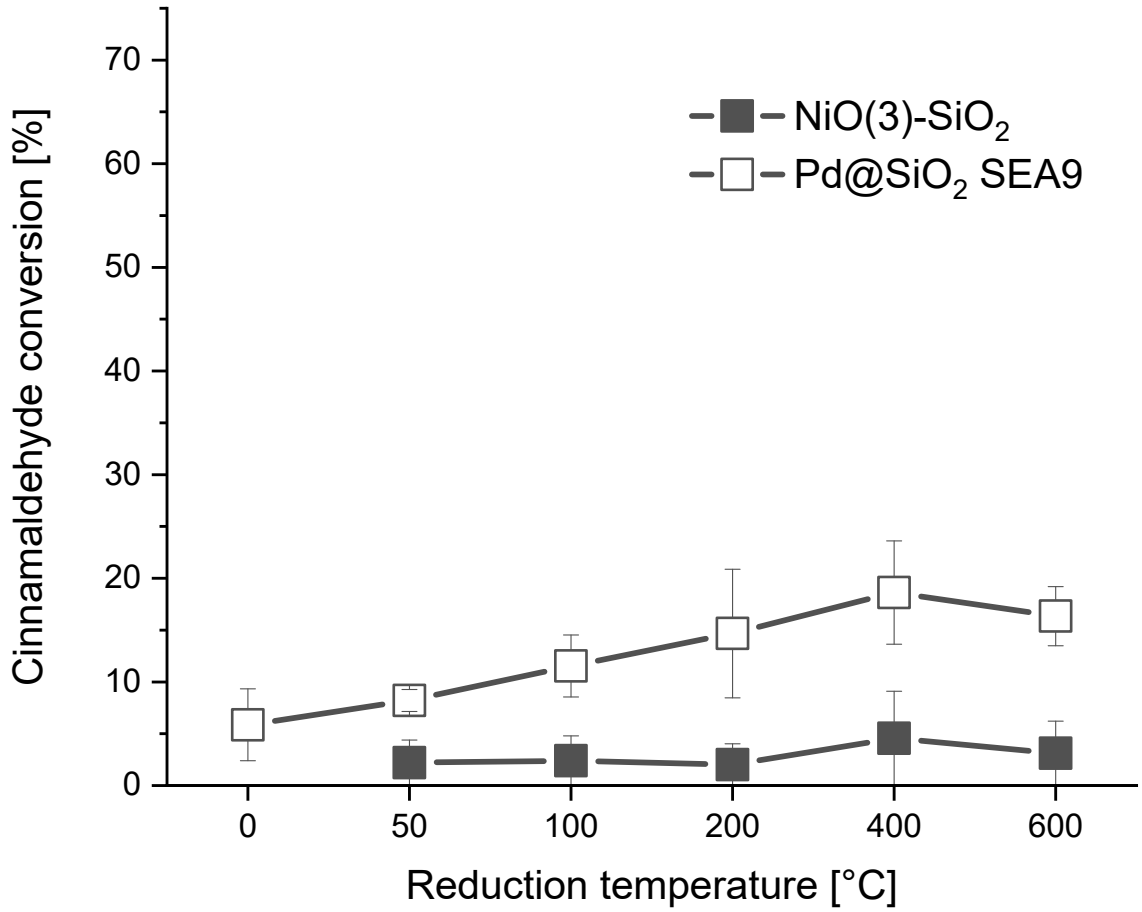

Figure S4. Cinnamaldehyde hydrogenation activity of $NiO(3)\text{-}SiO_2$ and $Pd@SiO_2$-SEA(9) (batch reactor, 50 °C, 4 mg catalyst, 2.8 ml IPA solvent, 1.2 ml cinnamaldehyde, 30 bar H_2, 10 h reaction time).

S5. Quasi in-situ XPS spectra of NiO(3)-SiO_2 after different reduction treatments.

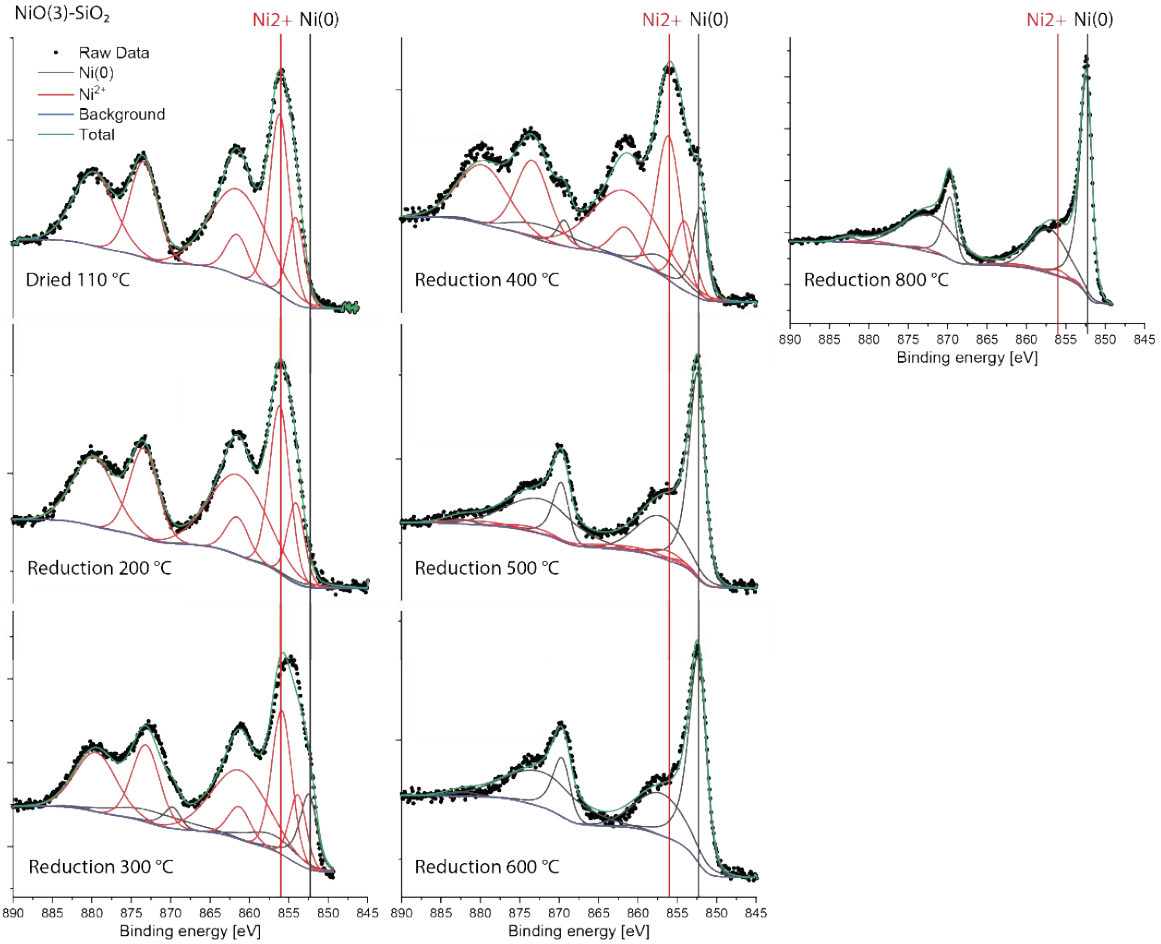

Figure S5. Quasi in-situ Ni 2p XPS spectra of NiO(3)-SiO_2.

S6. Ni 2p bulk reference spectra

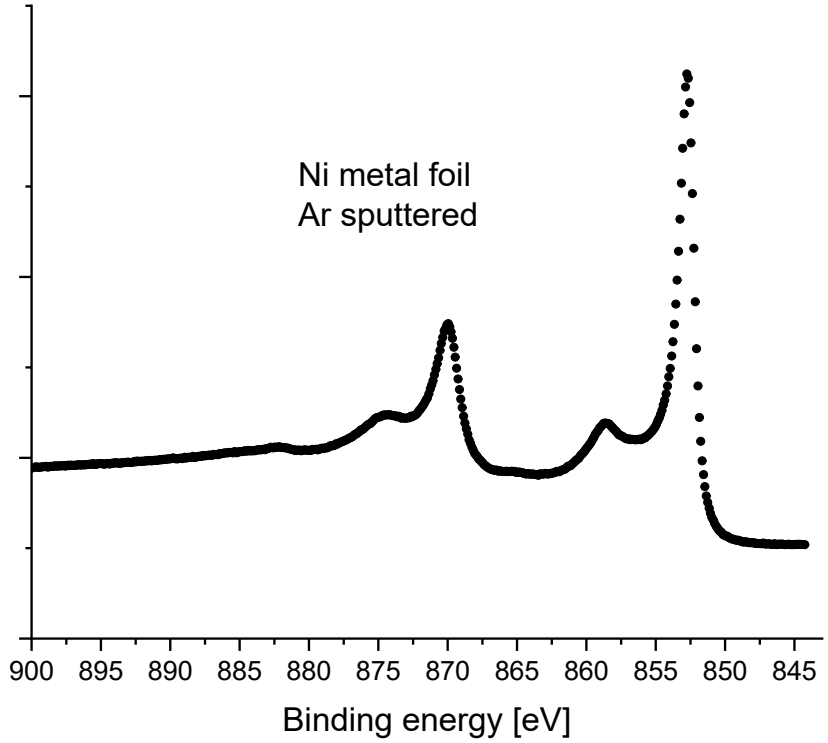

Figure S6. Ni 2p reference spectra of a Ni metal foil which was Ar sputtered to remove oxide layers.

S7. Quasi in-situ XPS of $NiO(3)\text{-}Pd@SiO_2$

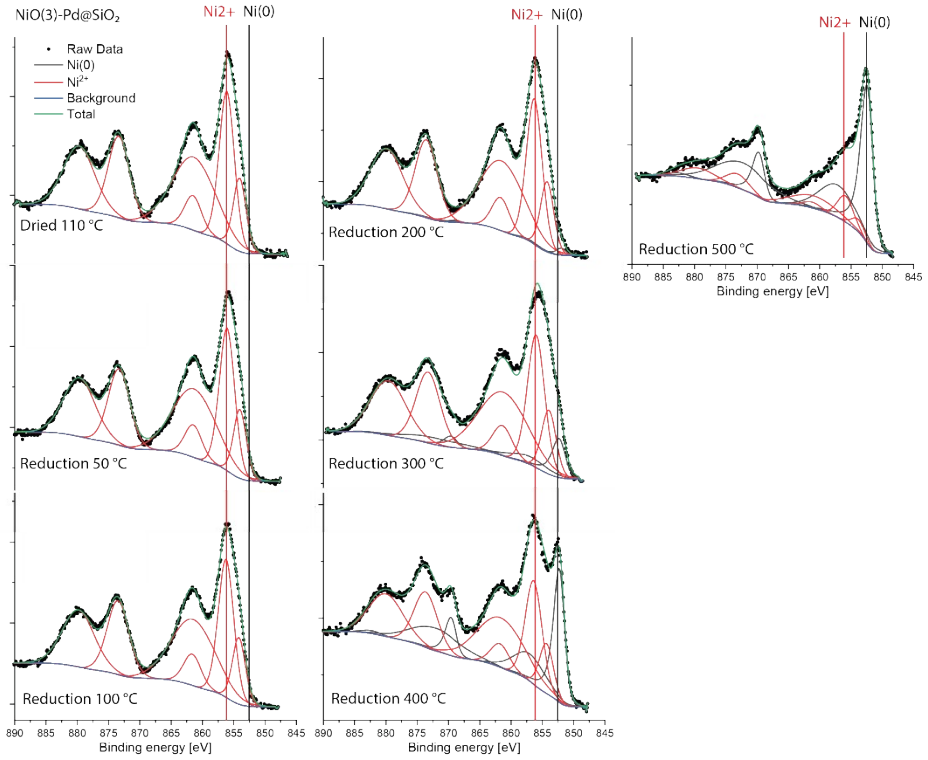

Figure S7. Quasi in-situ Ni 2p XPS spectra of $NiO(3)\text{-}Pd@SiO_2$.

S8. TPR with non-continuous heating rate

Temperature programed reduction (TPR) is carried out with temperature dwells instead of a continuous heating rate. Several peaks are observed at the different temperature dwells. These peaks are integrated and are used as the degree of reduction shown in Figure 9 in the main text. For the XPS data the percentages of Ni(0) in the Ni 2p fits of Pd@NiO(3)-SiO_2 (Fig. S10) and NiO(3)-Pd@SiO_2 (Fig. S8) are used. These values are plotted in Figure 8, where we can see that the TPR signals are quite similar, except slightly more reduction for NiO(3)-Pd@SiO_2 at low temperature, and more reduction for Pd@NiO(3)-SiO_2 at high temperature. Overall, we can see that there is a decent agreement between XPS and TPR, but that XPS lags the TPR data somewhat.

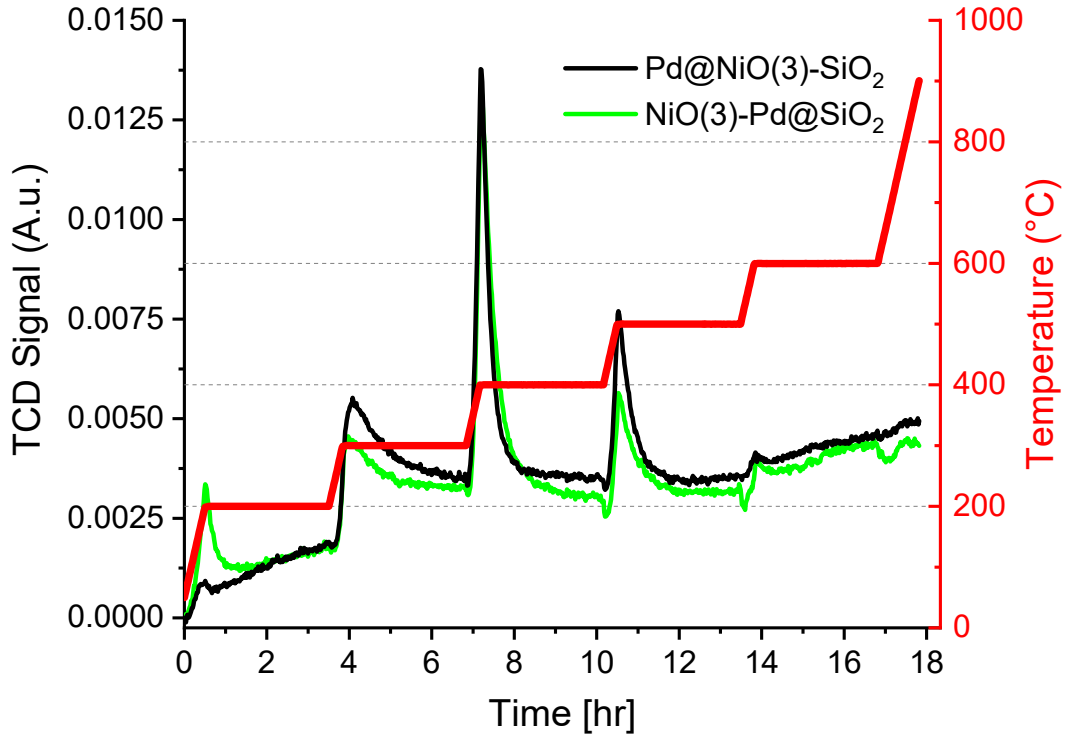

Figure S8. TPR of Pd@NiO(3)-SiO_2 and NiO(3)-Pd@SiO_2 measured with a non-linear temperature profile.

S9. Quasi in-situ XPS of Pd@NiO(3)-SiO_2

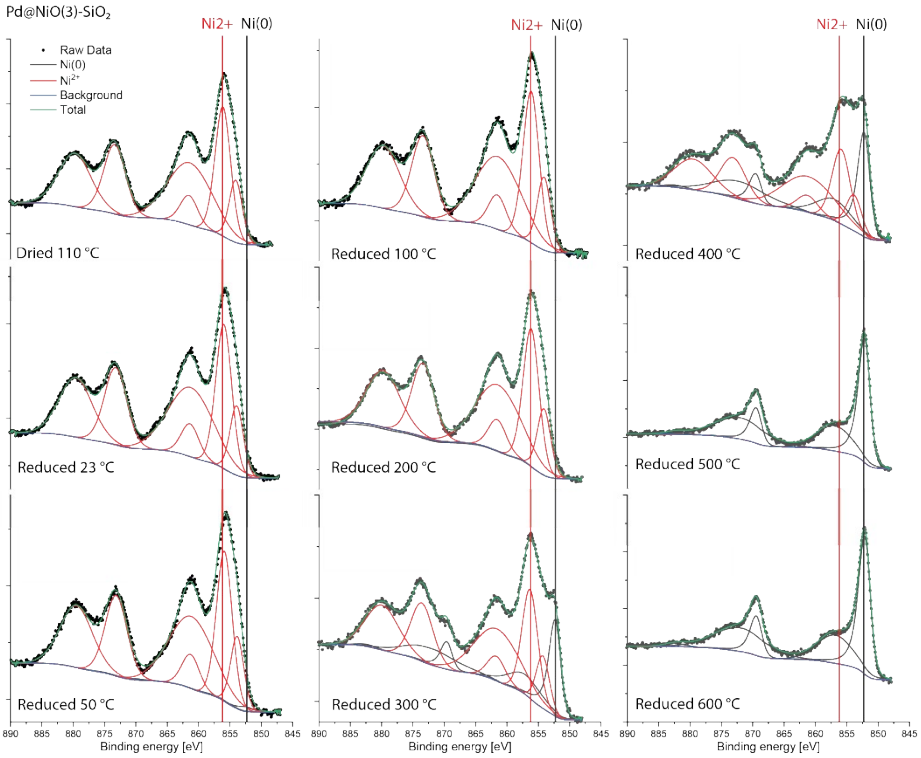

Figure S9. Quasi in-situ Ni 2p XPS spectra of Pd@NiO(3)-SiO_2.

S10. Reduction of PdO to Pd under RT CO atmosphere

A Pd@NiO(3)-SiO_2 sample was dried overnight and CO was dosed at RT. This showed peaks at 1991 and 1931 cm^{-1} which are indicative of linear and bridged bound CO on metallic Pd (Figure S10). The measurement was repeated on a fresh sample with the same pretreatment, but CO dosing was done under liquid nitrogen cooling (Figure S11). Here no signal of metallic Pd could be observed, showing that the CO at room temperature can reduce PdO and caused the formation of metallic Pd. This behavior was also observed in the literature [2].

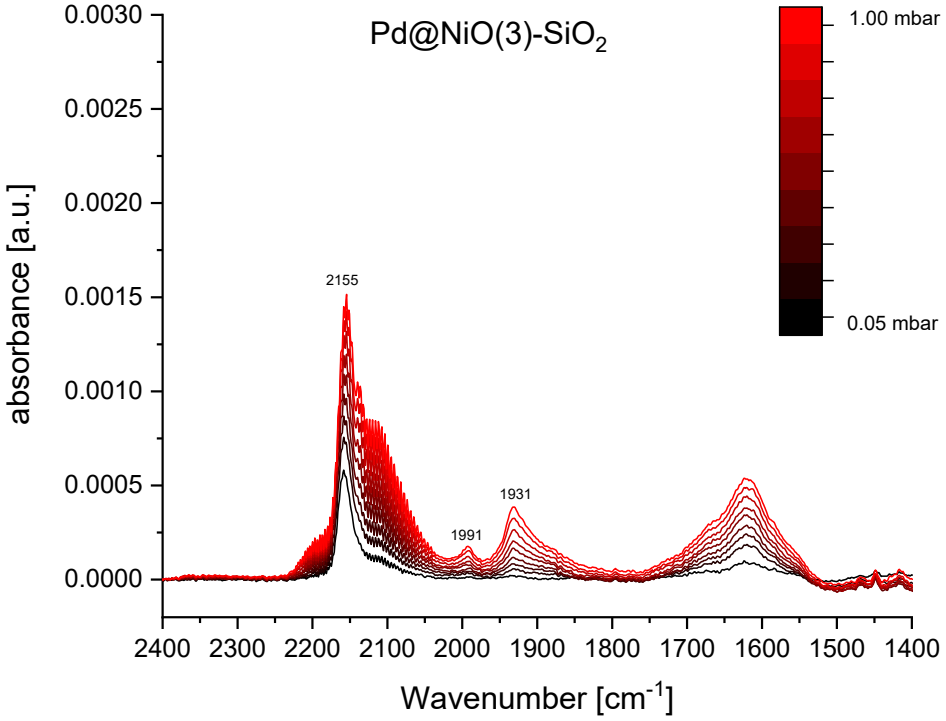

Figure S10. CO IR spectra of Pd@NiO(3)-SiO_2 dried at 110 °C measured at RT.

S11. CO-IR spectra of dried Pd@NiO(3)-SiO_2 without silica signal removal

The same sample and pretreatment as in Fig. S10. However, CO dosing was done under cooling at ~-170 °C. At these temperatures CO cannot reduce PdO and no CO bound to Pd can be seen. The spectra of blank silica (Fig. S12.) is subtracted from these spectra as described in the extended method S2.

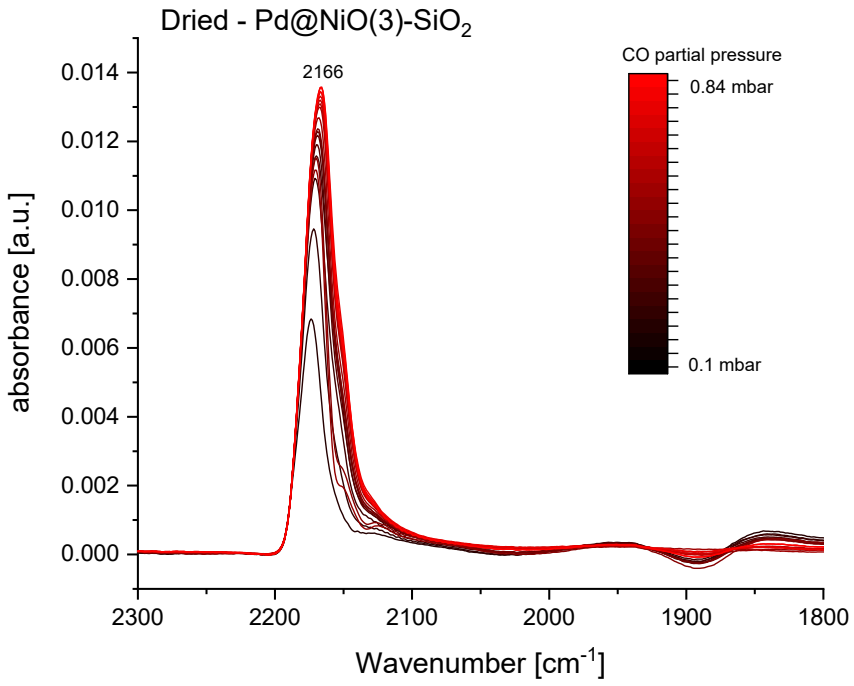

Figure S11. CO IR spectra of Pd@NiO(3)-SiO_2 acquired at ~-170 °C.

S12. CO-IR spectra of SiO_2 measured at ~-170 °C

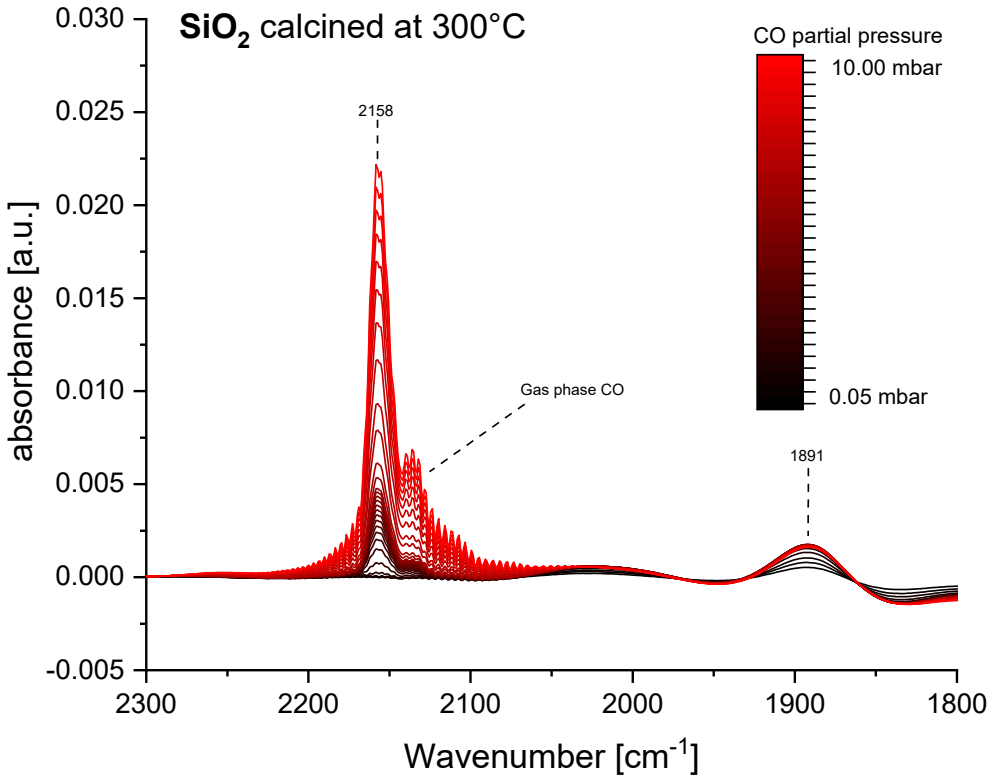

Figure S12. CO IR spectra of calcined silica measured at ~-170 °C.

S13. CO FTIR after different pretreatments with a CO pressure of 0.24 mbar.

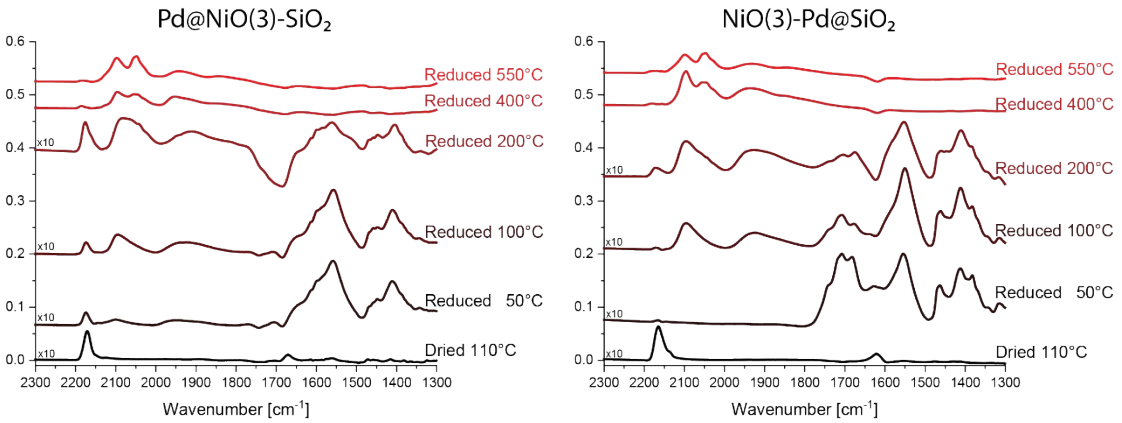

Figure S13. Larger domain of the CO IR spectra of Pd@NiO(3)-SiO$_2$ and NiO(3)-Pd@SiO$_2$ at 0.24 mbar CO partial pressure.

S14. CO-IR reference spectra of metallic Ni reduced at 400 °C. Silica and gas phase spectra are not subtracted in this figure.

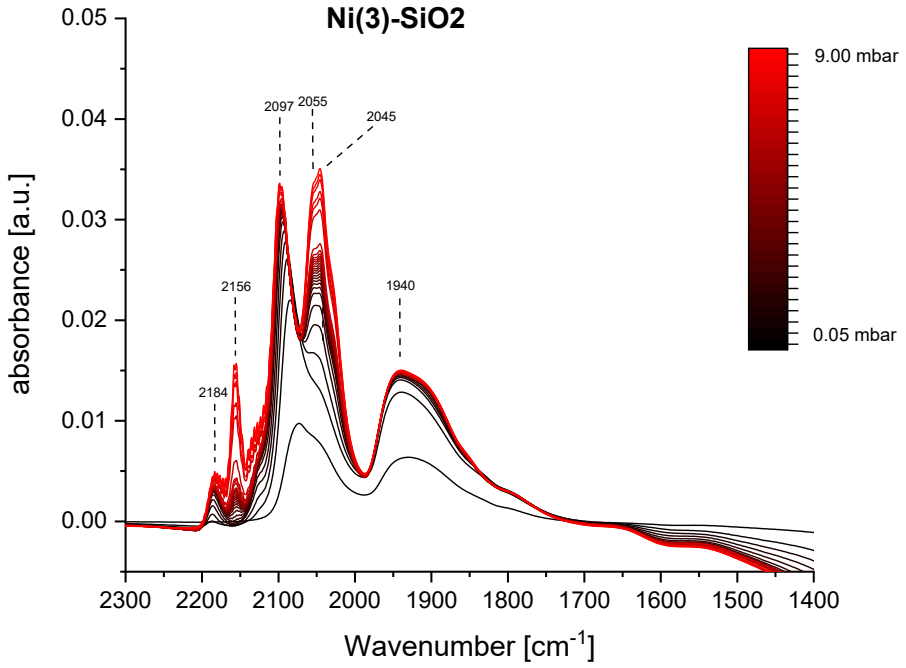

Figure S14. CO IR spectra of Ni(3)-SiO$_2$ reduced at 400 °C measured at ~-170 °C.

Table S1. H_2 chemisorption of Pd-NiO catalysts after different reduction treatments. * For the first data point the catalyst was dried in He. For the other points the catalyst was reduced at the indicated temperature in H_2. H:X ratios were based on the weight loadings of Pd and Ni as determined by ICP. In the case of bimetallic catalysts, both the H:Pd and H:Ni ratio was calculated. The H:Pd ratio at low reduction temperature is especially useful, as no NiO is reduced yet and we can assume that all hydrogen is adsorbed on Pd.

Sample name	Reduction temperature [°C]	1st H_2 Adsorption [mmol/gr_{cat}]	2nd H_2 Adsorption [mmol/gr_{cat}]	H:metal ratio, 1st adsorption	H:metal ratio, 2nd adsorption	H:Pd ratio, 1st adsorption	H:Pd ratio, 2nd adsorption	H:Ni ratio, 1st adsorption	H:Ni ratio, 2nd adsorption
Pd@NiO(3)-SiO_2	Dried 110*	0.085	0.033	0.110	0.043	3.614	1.413	0.113	0.044
	50	0.024	0.029	0.031	0.038	1.020	1.247	0.032	0.039
	100	0.032	0.030	0.041	0.039	1.360	1.285	0.043	0.040
	200	0.129	0.092	0.167	0.119	5.511	3.910	0.172	0.122
	300	0.236	0.181	0.305	0.234	10.061	7.707	0.315	0.241
	400	0.203	0.173	0.262	0.223	8.658	7.370	0.271	0.230
	550	0.216	0.160	0.278	0.207	9.180	6.817	0.287	0.213
NiO(3)-Pd@SiO_2	Dried 110*	0	0	0	0	0	0	0	0
	50	0.035	0.031	0.042	0.037	0.571	0.500	0.045	0.040
	100	0.073	0.057	0.087	0.068	1.181	0.919	0.094	0.073
	200	0.225	0.130	0.269	0.155	3.653	2.108	0.290	0.167
	300	0.343	0.224	0.409	0.267	5.567	3.636	0.442	0.289
	400	0.339	0.234	0.405	0.280	5.512	3.807	0.438	0.302
	550	0.268	0.196	0.321	0.234	4.359	3.181	0.346	0.253
Pd@SiO_2-SEA(9)	Dried 110*	0	0	0	0				
	50	0.016	0.015	0.676	0.646				
	100	0.025	0.024	1.060	1.007				
	200	0.021	0.022	0.895	0.926				
	300	0.028	0.025	1.161	1.049				
	400	0.032	0.022	1.347	0.905				
	550	0.026	0.020	1.069	0.819				
NiO(3)-SiO_2	Dried 110*	0	0	0	0				
	50	0	0	0	0				
	100	0	0	0	0				
	200	0.032	0	0.042	0				
	300	0.193	0.160	0.255	0.212				
	400	0.258	0.213	0.341	0.282				
	550	0.236	0.195	0.313	0.258				

References

[1] A. P. Grosvenor, M. C. Biesinger, R. S. C. Smart, and N. S. McIntyre, "New interpretations of XPS spectra of nickel metal and oxides," *Surf. Sci.*, vol. 600, no. 9, pp. 1771–1779, 2006.

[2] G. Spezzati *et al.*, "Atomically dispersed Pd-O species on CeO2(111) as highly active sites for low-temperature CO oxidation," *ACS Catal.*, vol. 7, no. 10, pp. 6887–6891, 2017.